NASA TECHNICAL NOTE

NASA TN D-3492

C. 1

LOAN COPY: RETURN TO
AFWL (WLIL-2)
KIRTLAND AFB, N MEX

TECH LIBRARY KAFB, NM
0130361

NASA TN D-3492

APPROXIMATION OF REENTRY ANGLES OF ATTACK FOR A SPINNING BODY FROM RATE-GYRO AND ACCELEROMETER DATA

RECEIVED
22 JUL 1966
Technical Library
AF Weapons
Laboratory

by Charles H. Whitlock

Langley Research Center
Langley Station, Hampton, Va.

NATIONAL AERONAUTICS AND SPACE ADMINISTRATION • WASHINGTON, D. C. • JULY 1966

TECH LIBRARY KAFB, NM
0130361

APPROXIMATION OF REENTRY ANGLES OF ATTACK FOR A SPINNING BODY FROM RATE-GYRO AND ACCELEROMETER DATA

By Charles H. Whitlock

Langley Research Center
Langley Station, Hampton, Va.

NATIONAL AERONAUTICS AND SPACE ADMINISTRATION

For sale by the Clearinghouse for Federal Scientific and Technical Information
Springfield, Virginia 22151 – Price $2.00

APPROXIMATION OF REENTRY ANGLES OF ATTACK FOR A SPINNING BODY FROM RATE-GYRO AND ACCELEROMETER DATA

By Charles H. Whitlock
Langley Research Center

SUMMARY

A technique for approximating reentry angles of attack from rate-gyro and accelerometer data is developed. The analysis is independent of initial conditions and mass and inertia terms, produces α and β as well as η histories, is independent of basic aerodynamic and trajectory parameters, and is workable around periods of lost data. The method is limited to spinning bodies having aerodynamic roll symmetry and assumes negligible-gravity, earth-rotation, and aerodynamic-damping-force effects. By use of an analytical simulation technique, the analysis is demonstrated with three typical reentry situations as examples. A portion of flight data is also analyzed, and the results are compared with those of another technique of analysis.

INTRODUCTION

One of the critical problem areas concerning ballistic rockets and satellite devices is their return to the earth's dense atmosphere from high-velocity, low-dynamic-pressure conditions in space. It is often necessary to evaluate the reentry motions of such spacecraft from flight data in order to adequately evaluate overall mission results. The purpose of this report is to present one technique by which the angular motions of an aerodynamically symmetric spacecraft may be approximated from body-fixed rate-gyro and accelerometer flight data.

Presently, there are several data-reduction techniques available for obtaining reentry motions from accelerometer and/or rate-gyro flight data. References 1 and 2 describe techniques by which both the rate-gyro and accelerometer time histories are used to determine both trajectory and motions histories. References 3 and 4 have presented a technique of analysis for determining angle-of-attack envelopes from only rate-gyro data. This analysis appears limited to known inertia properties. For many flights, particularly those of a research nature, it is desirable to evaluate flight data by a technique which is independent of mass and inertia variations. The elimination of prior knowledge of initial conditions and trajectory parameters is also useful. By extending

the results of reference 3 to include accelerometer data, a technique is developed by which spacecraft angle-of-attack motions during reentry may be rapidly approximated without knowledge of aerodynamic parameters or spacecraft physical properties. The technique is tested for validity by application to three simulated flight situations. Finally a portion of actual flight data is evaluated and the results compared with those obtained in reference 2.

This report includes an appendix by John D. Shaughnessy, of the Langley Research Center, which presents the transformation of the equations of translational motion from inertial to geodetic or local horizontal reference.

SYMBOLS

a_X, a_Y, a_Z linear accelerations (due to external forces) at center of gravity along body axes, g units (1g = 9.807 meters per second^2)

C_R force coefficient in plane defined by relative velocity vector and X-axis

G_X, G_Y, G_Z force components along body axes due to gravity

g acceleration due to force of gravity, feet per second^2 (meters per second^2)

h altitude, feet (meters)

L north latitude measured positive from equatorial plane, degrees or radians

l_i, m_i, n_i Euler angle direction cosines between spacecraft body-axis system and local gravity-axis system

m mass, slugs (kilograms)

p rolling velocity, radians per second

q pitching velocity, radians per second

q' dynamic pressure, pounds per foot^2 (newtons per meter^2)

R spherical earth radius, 20.924640×10^6 feet (6.378×10^6 meters)

r yawing velocity, radians per second

S	body frontal area, feet^2 (meters^2)
u,v,w	component of inertial velocity along X-, Y-, and Z-axis, respectively, feet per second (meters per second)
V	total inertial velocity, feet per second (meters per second)
V_R	component of velocity due to earth rotation, feet per second (meters per second)
W	weight, pounds (newtons)
X,Y,Z	body-axis system (origin at center of gravity)
α	angle of attack, radians unless otherwise noted
β	angle of sideslip, radians unless otherwise noted
ϵ	angle defining the plane of the resultant flow incidence angle with respect to the body-fixed axes, arc tan $\bar{w}/\bar{v}$, radians unless otherwise noted
η	resultant or total flow incidence angle, radians unless otherwise noted
λ	west longitude measured negative from Greenwich meridian, degrees or radians
ω_e	angular velocity of rotating earth, 7.292115×10^{-5} radian per second
θ,ψ,ϕ	spacecraft attitude angles relative to gravity-axis system, radians or degrees
Δ	incremental change in a quantity

Dots over symbols denote differentiation with respect to time.

Bars over symbols denote earth-relative quantities.

ANALYTICAL ANALYSIS

Mathematical Development

If aerodynamic-damping-force effects are neglected, the force equations along the body-fixed Y- and Z-axes (fig. 1) of an aerodynamically symmetric reentry body may be expressed as:

$$m(\dot{v} - wp + ur) = -C_R q'S \cos \epsilon + G_Y \tag{1}$$

$$m(\dot{w} - uq + vp) = -C_R q'S \sin \epsilon + G_Z \tag{2}$$

As used in references 1 and 2, equations (1) and (2) may be expressed as:

$$m(\dot{v} - wp + ur) = Wa_Y + G_Y \tag{3}$$

$$m(\dot{w} - uq + vp) = Wa_Z + G_Z \tag{4}$$

or

$$Wa_Y = -C_R q'S \cos \epsilon \tag{5}$$

$$Wa_Z = -C_R q'S \sin \epsilon \tag{6}$$

Combining equations (5) and (6),

$$\tan \epsilon = \frac{-a_Z}{-a_Y} \tag{7}$$

The quadrant of ϵ can be assessed by testing the numerator and denominator (keeping negative signs) of equation (7).

From the geometry of figure 1, it can be seen that

$$\overline{u} = \overline{V} \cos \eta \tag{8}$$

$$\overline{v} = \overline{V} \sin \eta \cos \epsilon \tag{9}$$

$$\overline{w} = \overline{V} \sin \eta \sin \epsilon \tag{10}$$

Taking the time derivative of equations (9) and (10) and combining the results, the following is obtained (in terms of earth-relative velocities):

$$\dot{\epsilon} = \frac{-\dot{\overline{v}} \sin \epsilon + \dot{\overline{w}} \cos \epsilon}{\overline{V} \sin \eta} \tag{11}$$

The equations of motion may be written in terms of a geodetic or earth-relative axis system by expressing both the inertial velocities and rates of change of inertial velocity in terms of earth-relative velocities and earth-rotation terms. Details of the

transformation are presented in the appendix. An order-of-magnitude analysis of the various quantities associated with this transformation indicates that the effects of earth-rotation are negligible for a typical reentry. With these results, equations (1) and (2) may be approximated as:

$$m\left(\dot{\bar{v}} - \bar{w}p + \bar{u}r\right) = -C_R q'S \cos \epsilon + G_Y \tag{12}$$

$$m\left(\dot{\bar{w}} - \bar{u}q + \bar{v}p\right) = -C_R q'S \sin \epsilon + G_Z \tag{13}$$

Rearranging and neglecting gravity effects,

$$\dot{\bar{v}} = \bar{w}p - \bar{u}r - \frac{C_R q'S}{m} \cos \epsilon \tag{14}$$

$$\dot{\bar{w}} = \bar{u}q - \bar{v}p - \frac{C_R q'S}{m} \sin \epsilon \tag{15}$$

Substituting equations (14), (15), (8), (9), and (10) into equation (11) gives:

$$\tan \eta = \frac{r \sin \epsilon + q \cos \epsilon}{p + \dot{\epsilon}} \tag{16}$$

This equation is identical to the results of reference 3. The quadrant of η can be obtained by knowing the direction of flight (whether forward or backward).

For the particular aerodynamic angle system shown in figure 1, the angles of attack and sideslip may be written as

$$\tan \alpha = \frac{\bar{w}}{\bar{u}} = \tan \eta \sin \epsilon \tag{17}$$

$$\sin \beta = \frac{\bar{v}}{\bar{V}} = \sin \eta \cos \epsilon \tag{18}$$

Equations (7), (16), (17), and (18) allow the determination of ϵ, η, α, and β from body-fixed angular rate and accelerometer data. All processes used involve algebra and differentiation of data histories; hence, the process is independent of integration or initial condition constants. However, sufficient portions of the data histories must be available such that an ϵ history can be constructed and values of $\dot{\epsilon}$ obtained by measuring slopes of ϵ. Values of $\dot{\epsilon}$ may also be obtained from

$$\dot{\epsilon} = \frac{\dot{a}_Z - \frac{a_Z}{a_Y} \dot{a}_Y}{a_Y \left[1 + \left(\frac{a_Z}{a_Y}\right)^2\right]} \tag{19}$$

This expression is obtained by differentation of equation (7). Time derivatives of both the a_Y and a_Z histories are required. For the example situations to be presented, final $\dot{\epsilon}$ histories were obtained by fairing a smooth curve over the combined results by both techniques.

Technique Limitations

An approximate solution of the equations of motion has allowed a technique to be developed for obtaining angles of attack during reentry from body-fixed rate-gyro and accelerometer histories. The analysis is limited to reentry spacecraft which are aerodynamically symmetric about the longitudinal axis. Only the force equations of motion are utilized; hence, the technique is applicable to spacecraft with center-of-gravity displacements off the longitudinal axis, provided the accelerations at that center of gravity can be determined. (In this case the asymmetries are introduced into the moment equations of motion as indicated in ref. 5.) The instrumentation axes must be alined with the longitudinal axis of aerodynamic symmetry, however. Aerodynamic damping forces (but not moments) have also been neglected. These limitations allow the determination of the aerodynamic phase angle ϵ at any instant of time from flight accelerometer data. By neglecting gravity and earth-rotation effects, an expression has been obtained for the resultant flow incidence angle η in terms of p, q, r, ϵ, and $\dot{\epsilon}$. Previous investigations have indicated that angular motion about the velocity vector during reentry is affected little by gravity over short periods of time. The order of magnitude analysis of the appendix indicates that earth-rotation terms are negligible for a typical reentry.

In an effort to define further limitations on the analysis, a first-order approximation of the errors introduced into η from inaccuracies of input quantities yields the following result (from eq. (16)):

$$\Delta\eta = \left[\frac{(\sin\epsilon)\Delta r + (\cos\epsilon)\Delta q + (r\cos\epsilon - q\sin\epsilon)\Delta\epsilon}{(p+\dot{\epsilon}) + \dfrac{(r\sin\epsilon + q\cos\epsilon)^2}{(p+\dot{\epsilon})}}\right] - \left[\frac{\Delta p + \Delta\dot{\epsilon}}{(r\sin\epsilon + q\cos\epsilon) + \dfrac{(p+\dot{\epsilon})^2}{(r\sin\epsilon + q\cos\epsilon)}}\right] \tag{20}$$

From equation (20), it is seen that whenever the denominator of the coefficients of the error quantities approaches zero, then minute errors in r, q, ϵ, p, or $\dot{\epsilon}$ produce very large errors in η. This condition can occur only when $p + \dot{\epsilon} \approx 0$ and $r\sin\epsilon + q\cos\epsilon \approx 0$ simultaneously. Unreliable results are expected to be obtained

whenever this situation is encountered. If the results of equation (7) are applied, error amplification may occur whenever

$$\frac{-a_Z}{-a_Y} \approx -\frac{q}{r} \tag{21}$$

and

$$p \approx -\dot{\epsilon} \tag{22}$$

It appears that the reliability of the analysis can be tested with actual flight data by comparing the $-q/r$ and $-a_Z/-a_Y$ histories first and then the $-p$ and $\dot{\epsilon}$ results. When the curves approach or cross, large errors in the resultant angle of attack η may be expected.

The validity of the assumptions and limitations described herein will be tested with the use of an analytical simulation technique (more fully described in the next section). In addition to these quantities, the effects of random scatter in the input data are included. Accelerometer and rate-gyro histories (to 5 significant figures) are obtained from a solution to the six-degree-of-freedom equations of motion by the electronic digital process of reference 5. (The particular program utilized assumes an oblate rotating earth.) In order to simulate flight data, the accelerometer and gyro values are rounded off to two significant figures and used as inputs to the data reduction technique. For example, a typical gyro value obtained from the six-degree-of-freedom solution (hereinafter referred to as the 6-D solution) might be 8.17738 rad/sec. This value would be read into the data reduction process as 8.2 rad/sec. A comparison of the angles of attack obtained from the "flight" data with those of the 6-D solution gives an indication of the output errors involved due to the assumptions herein and input data accurate to only two significant figures. An investigation into the effects of aerodynamic asymmetries is not included in this analysis.

DATA REDUCTION AND MOTION COMPARISON

The validity of the data reduction technique described herein is tested, three typical reentry situations being used as examples. For each example (called cases 1, 2, and 3, respectively), reentry body physical properties and initial flight conditions are used as inputs to the solution of the six equations of motion (ref. 5). Aerodynamic parameters, mass, and inertia histories along with initial values of altitude, velocity, and spacecraft orientation angles are assumed. Reentry trajectories are then "flown" on the computer. From this 6-D solution, values of p, q, r, a_Y, and a_Z and α, β, and η histories are obtained. The values of p, q, r, a_Y, and a_Z are rounded off to two significant figures (as noted in the previous section) and used as inputs to the data reduction process. The values of α, β, and η obtained from the reduction of these "flight"

data are then compared with those values obtained from the 6-D solution. The three reentry situations chosen for analysis are similar to typical research flight tests. Arbitrary values for initial disturbances are assumed in all cases and have no relation to any previous flight test. Finally, a portion of actual flight data from reference 2 is reduced and the motions compared with those of that publication. Each case is considered separately and the results discussed in a later section.

Case 1

For case 1, a wide-angle conical reentry configuration was assumed to be flying in a trajectory of steep flight-path angle (-84°) with an entry velocity of 21 000 ft/sec (6400.8 m/sec). Typical initial conditions with a high spin rate ($p = 87$ rad/sec) were assumed, and a trajectory during reentry was generated. With the use of this trajectory, short histories of p, q, r, a_Y, and a_Z were recorded at 11 sec for use in the data reduction process. Table I shows a sample of these values. With these data used, time histories of $-a_Z/-a_Y$ and $-q/r$ are shown in figure 2. As expected, each half-cycle movement of ϵ causes $-a_Z/-a_Y$ to vary from $-\infty$ to $+\infty$. For the particular motion of case 1, the histories of $-q/r$ do not appear to cross the $-a_Z/-a_Y$ histories (except near infinity). Histories of ϵ were obtained from equation (7) and values of $\dot{\epsilon}$ were obtained by taking slopes of the ϵ history and from equation (19). Figure 3 presents both the ϵ and final $\dot{\epsilon}$ histories. This chart indicates that the $\dot{\epsilon}$ and $-p$ histories do not approach or cross over the time period being analyzed; hence, the data reduction process is expected not to produce erratic results. The angles η, α, and β were calculated with the use of equations (16), (17), and (18) and are presented in figure 4. Also shown are the values obtained from the original 6-D solutions for the equations of motion.

Case 2

The reentry body for case 2 was assumed to be an Apollo-type configuration flying in a trajectory of shallow flight-path angle (-15°) with an entry velocity of 38 000 ft/sec (11 582.4 m/sec). The center of gravity was located on the longitudinal axis for this case. As in case 1, with typical initial conditions and spacecraft physical properties, a reentry trajectory was generated on the computer. A spin rate of 19 rad/sec was assumed. Histories of p, q, r, a_Y, and a_Z were extracted over a short time period at 1678 sec (table II) for use in the data reduction technique. Comparison of the $-a_Z/-a_Y$ and $-q/r$ histories from these data is shown in figure 5. Figure 6 presents the ϵ and final $\dot{\epsilon}$ histories over the time period. From these two figures, it is observed that the conditions of $\frac{-a_Z}{-a_Y} \approx -\frac{q}{r}$ and $\dot{\epsilon} \approx -p$ are encountered simultaneously in several instances; hence, the results are expected to be erratic at these times. Figure 7 presents the α,

β, and η histories obtained from both the data reduction process and the 6-D solutions to the equations of motion.

Case 3

The analytical situation selected for case 3 was similar to that of case 2. An identical configuration and reentry trajectory were assumed. In this case, a center-of-gravity location off the longitudinal axis was used. The offset center of gravity was located such that a trim angle of attack of approximately 10° in the negative α-direction was produced by the asymmetry. Table III presents the sample of data selected (at 1678 sec) for analysis. Figure 8 presents the comparison of the $-a_Z/-a_Y$ and $-q/r$ histories, and figure 9 shows the ϵ and final $\dot{\epsilon}$ values. The conditions for error amplification are encountered twice over the time interval. Figure 10 presents the α, β, and η histories obtained for case 3.

Flight Results

As a further test of the data reduction technique, the same reentry flight data as used in reference 2 were used as inputs to the process. Table IV presents a portion of these accelerometer and rate-gyro data during the time interval chosen for analysis. These are the final smooth data that were used in the integration method of analysis of that publication. With these quantities being used, the comparison of the $-a_Z/-a_Y$ and $-q/r$ histories is shown in figure 11. Figure 12 presents the ϵ and final $\dot{\epsilon}$ histories, and figure 13 shows the reduced and faired values for α, β, and η. Also shown is the resultant angle-of-attack history from reference 2. From the accelerometer data and spacecraft physical properties and dynamic pressure histories from reference 2, a time history of C_R was calculated by the methods of that publication (eq. (A16)). Cross-plotting these values with those from the faired η history of figure 13 produces the curve for C_R plotted against η presented in figure 14. Also shown are the results from reference 2.

RESULTS AND DISCUSSION

Analysis has indicated that simultaneous conditions of $\frac{-a_Z}{-a_Y} \approx -\frac{q}{r}$ and $\dot{\epsilon} \approx -p$ can produce excessive errors in the data reduction technique described herein. For case 1 the motions were such that error amplification conditions were not encountered, and the results show that the reduced data were always within a few degrees of the 6-D values (fig. 4). Errors in α and β result from inaccuracies in η, but their oscillatory nature gives the illusion of better agreement. In cases 2 and 3, however, these conditions for error amplification were encountered in several instances. At these times, the data reduction technique produced erratic results (figs. 7 and 10) due to small errors in the input quantities (two significant figure accuracy) and in fairing the $\dot{\epsilon}$ history. In

both cases, the reduced data showed reasonable agreement with the original 6-D histories over the remainder of the time intervals being analyzed. For a flight situation of this type, reference to the $-a_Z/-a_Y$, $-q/r$, $\dot{\epsilon}$, and $-p$ histories would be necessary to determine which points were of questionable accuracy. By fairing first the α and β curves with the use of reliable data points, the η history fairing can be more easily obtained. Comparison of the accuracies obtained from cases 1 and 2 (when error amplification is not present) indicates that the method described herein produces reasonable results for vehicle spin rates and velocities typical of reentry research experiments. For the case of zero spin rate ($\dot{\epsilon} = -p = 0$), the technique of analysis is not applicable. Comparison of case 2 and case 3 results indicates that equivalent accuracies are obtained for the center of gravity either on or off the longitudinal axis. It is required that the accelerations used be those at the displaced center of gravity, however.

A portion of the flight data of reference 2 was analyzed with the methods described herein. Comparison of the $-q/r$ with the $-a_Z/-a_Y$ histories and the $\dot{\epsilon}$ with the $-p$ calculations indicates that the analysis should not produce erratic results over the time interval chosen for analysis. Figure 13 shows that although the reduced data do not agree with the results of reference 2, the maximum and minimum values of η are of the same magnitude. For the time period 443.81 to 444.35 sec, the cross-plots of C_R against η (fig. 14) show that neither angle-of-attack history agrees with wind-tunnel derived results. As noted in reference 2, configuration changes due to heat-shield ablation may account for the disagreement with wind-tunnel values. Differences between the two techniques of analysis could not be resolved.

CONCLUDING REMARKS

A technique has been developed for rapidly approximating reentry angles of attack for a spinning vehicle from onboard rate gyro and accelerometer data. The technique is independent of initial conditions and mass and inertia values, produces α and β as well as η histories, is independent of basic aerodynamic and trajectory parameters, and is workable around periods of lost data. The method assumes aerodynamically symmetric bodies and negligible-gravity and earth-rotation effects. Aerodynamic damping forces are also neglected. It is believed that this type of analysis may be useful in approximating reentry angle-of-attack histories during the atmospheric portion of reentry when either trajectory data, dynamic pressures, aerodynamic parameters, inertia properties, or spatial orientation are not known precisely.

Langley Research Center,
National Aeronautics and Space Administration,
Langley Station, Hampton, Va., March 29, 1966.

APPENDIX

TRANSFORMATION OF EQUATIONS OF TRANSLATIONAL MOTION FROM INERTIAL TO GEODETIC OR LOCAL HORIZONTAL REFERENCE

By John D. Shaughnessy

The translational equations of motion for a rigid vehicle having six degrees of freedom are (ref. 2):

$$\left.\begin{aligned} \dot{u} + wq - vr &= ga_X + g\ell_3 \\ \dot{v} + ur - wp &= ga_Y + gm_3 \\ \dot{w} - uq + vp &= ga_Z + gn_3 \end{aligned}\right\} \tag{A1}$$

where u, v, and w are the body-axis components of the inertial velocity of the vehicle. Equations (A1) can be referenced to the local gravity axes by introducing the following equations (direction cosines are relative to the geodetic axes, ref. 2):

$$\left.\begin{aligned} u &= \bar{u} + \ell_1(R + h)\omega_e \cos L \\ v &= \bar{v} + m_1(R + h)\omega_e \cos L \\ w &= \bar{w} + n_1(R + h)\omega_e \cos L \end{aligned}\right\} \tag{A2}$$

If

$$E = (R + h)\omega_e \cos L \tag{A3}$$

the time derivative of equations (A2) may be written as,

$$\left.\begin{aligned} \dot{u} &= \dot{\bar{u}} + \dot{\ell}_1 E + \ell_1 \dot{E} \\ \dot{v} &= \dot{\bar{v}} + \dot{m}_1 E + m_1 \dot{E} \\ \dot{w} &= \dot{\bar{w}} + \dot{n}_1 E + n_1 \dot{E} \end{aligned}\right\} \tag{A4}$$

Also from reference 2,

$$\left.\begin{aligned} \ell_1 &= \cos\theta \cos\psi \\ \ell_2 &= \cos\theta \sin\psi \\ \ell_3 &= -\sin\theta \\ m_1 &= \sin\theta \sin\phi \cos\psi - \cos\phi \sin\psi \\ m_2 &= \sin\theta \sin\phi \sin\psi + \cos\phi \cos\psi \end{aligned}\right\} \tag{A5}$$

(Equations continued on next page)

APPENDIX

$$\left.\begin{aligned} m_3 &= \cos\theta \sin\phi \\ n_1 &= \sin\theta \cos\phi \cos\psi + \sin\phi \sin\psi \\ n_2 &= \sin\theta \cos\phi \sin\psi - \sin\phi \cos\psi \\ n_3 &= \cos\theta \cos\phi \end{aligned}\right\} \tag{A5}$$

and

$$\left.\begin{aligned} \dot{\psi} &= \frac{r \cos\phi + q \sin\phi}{\cos\theta} + K_\psi \\ \dot{\theta} &= q \cos\phi - r \sin\phi - K_\theta \\ \dot{\phi} &= p + r \tan\theta \cos\phi + q \tan\theta \sin\phi + K_\phi + K_\psi \sin\theta \end{aligned}\right\} \tag{A6}$$

where K_ψ, K_θ, and K_ϕ are the body-axis components of the absolute angular velocity of the geodetic axis system moving with the vehicle and are given by

$$\left.\begin{aligned} K_\psi &= \dot{L} \cos\psi \tan\theta + \left(\omega_e + \dot{\lambda}\right)(\sin L + \cos L \sin\psi \tan\theta) \\ K_\theta &= \dot{L} \sin\psi - \left(\omega_e + \dot{\lambda}\right)\cos L \cos\psi \\ K_\phi &= \dot{L} \frac{\cos\psi}{\cos\theta} + \left(\omega_e + \dot{\lambda}\right)\cos L \frac{\sin\psi}{\cos\theta} \end{aligned}\right\} \tag{A7}$$

The time derivatives of l_1, m_1, and n_1 are determined as follows:

$$\dot{l}_1 = -\dot{\theta} \sin\theta \cos\psi - \dot{\psi} \cos\theta \sin\psi \tag{A8}$$

Substituting equations (A6) into equation (A8) and rearranging gives

$$\begin{aligned} \dot{l}_1 = {} & r(\sin\theta \sin\phi \cos\psi - \cos\phi \sin\psi) - q(\sin\theta \cos\phi \cos\psi + \sin\phi \sin\psi) \\ & + K_\theta \sin\theta \cos\psi - K_\psi \cos\theta \sin\psi \end{aligned} \tag{A9}$$

With the use of equations (A5), equation (A9) may be written in the following form:

$$\dot{l}_1 = r m_1 - q n_1 + K_\theta \sin\theta \cos\psi - l_2 K_\psi \tag{A10}$$

In a similar manner $\dot{m}_1$ and $\dot{n}_1$ are obtained as follows:

$$\dot{m}_1 = p n_1 - r l_1 - l_1 \sin\phi K_\theta + \left(n_1 \sin\theta - m_2\right)K_\psi + n_1 K_\phi \tag{A11}$$

$$\dot{n}_1 = q l_1 - p m_1 - l_1 \cos\phi K_\theta - \left(m_1 \sin\theta + n_2\right)K_\psi - m_1 K_\phi \tag{A12}$$

APPENDIX

With the use of equations (A10), (A11), and (A12), equations (A4) become

$$\left.\begin{aligned}
\dot{u} &= \dot{\bar{u}} + \left(rm_1 - qn_1 + \sin\theta\cos\psi\, K_\theta - l_2 K_\psi\right)E + l_1\dot{E} \\
\dot{v} &= \dot{\bar{v}} + \left[pn_1 - rl_1 - l_1\sin\phi\, K_\theta + \left(n_1\sin\theta - m_2\right)K_\psi + n_1 K_\phi\right]E + m_1\dot{E} \\
\dot{w} &= \dot{\bar{w}} + \left[ql_1 - pm_1 - l_1\cos\phi\, K_\theta - \left(m_1\sin\theta + n_2\right)K_\psi - m_1 K_\phi\right]E + n_1\dot{E}
\end{aligned}\right\} \qquad \text{(A13)}$$

Substituting equations (A2) and (A13) into equations (A1) and simplifying with the aid of equation (A3) gives

$$\left.\begin{aligned}
\dot{\bar{u}} + \bar{w}q - \bar{v}r &= ga_X + gl_3 + \left(l_2 K_\psi - \sin\theta\cos\psi\, K_\theta\right)E - l_1\dot{E} \\
\dot{\bar{v}} + \bar{u}r - \bar{w}p &= ga_Y + gm_3 + \left[\left(m_2 - n_1\sin\theta\right)K_\psi + l_1\sin\phi\, K_\theta - n_1 K_\phi\right]E - m_1\dot{E} \\
\dot{\bar{w}} - \bar{u}q + \bar{v}p &= ga_Z + gn_3 + \left[\left(n_2 - m_1\sin\theta\right)K_\psi + l_1\cos\phi\, K_\theta + m_1 K_\phi\right]E - n_1\dot{E}
\end{aligned}\right\} \qquad \text{(A14)}$$

Equations (A14) are the equations of translational motion written in terms of the earth-relative velocity components. The terms on the right-hand side involving E and $\dot{E}$ are the earth's rotation terms and make equations (A14) and (A1) equivalent. For a typical ballistic Earth reentry, $\dot{E}$ is on the order of unity and E is on the order of 10^3, whereas the terms in parentheses are on the order of 10^{-3} and the direction cosines are at most on the order of unity. Thus, the maximum values of the E and $\dot{E}$ terms are approximately one order of magnitude smaller than the maximum values of the gravity terms and during reentry may be several orders of magnitude smaller than the external force terms.

REFERENCES

1. Lovelace, Uriel M.; Hoffman, Sherwood; and Mayhue, Robert J.: Analysis of the Trajectory and Large-Amplitude Motions of a Scout Vehicle During Fourth-Stage Reentry Flight. NASA TN D-2309, 1964.

2. Mayhue, Robert J.: Determination of Trajectory and Angles of Attack of a Scout Heat-Transfer Spacecraft During Reentry Flight in the Atmosphere. NASA TN D-2776, 1965.

3. Nelson, Edward O.: Angle of Attack From Body Fixed Rate Gyros. LMSC AO34132, Lockheed Missiles and Space Co., Aug. 20, 1963.

4. Nelson, Edward O.: Angle of Attack From Body-Fixed Rate Gyros. AIAA J. (Tech. Notes), vol. 2, no. 7, July 1964, pp. 1324-1325.

5. Dennison, A. J.; and Butler, J. F.: Missile and Satellite Systems Program For the I.B.M. 7090. Tech. Inform. Ser. No. 61 SD 170, Missile and Space Vehicle Dept., Gen. Elec. Co., Feb. 1962.

TABLE I.- SAMPLE OF "FLIGHT" DATA FOR CASE 1

Time, sec	a_Y, g units	a_Z, g units	p, rad/sec	q, rad/sec	r, rad/sec
11.0206	2.3	-3.9	-87	-1.6	1.8
11.0256	3.9	-2.3	-87	-2.7	.7
11.0306	4.4	-.1	-87	-3.1	-1.0
11.0356	3.8	2.1	-87	-2.7	-2.6
11.0406	2.1	3.7	-87	-1.4	-3.7
11.0456	-.1	4.2	-87	.2	-4.1
11.0506	-2.3	3.5	-87	1.8	-3.6
11.0556	-3.9	1.8	-87	3.0	-2.4
11.0606	-4.4	-.4	-87	3.4	-.7
11.0656	-3.7	-2.6	-87	2.8	.9
11.0706	-2.0	-4.2	-87	1.5	2.1
11.0756	.2	-4.7	-87	-.1	2.4
11.0806	2.5	-4.0	-87	-1.8	1.9
11.0856	4.0	-2.3	-87	-3.0	.6
11.0903	4.5	-.1	-87	-3.3	-.1
11.0953	3.9	2.2	-87	-2.8	-2.7
11.1003	2.1	3.8	-87	-1.5	-3.8
11.1053	-.2	4.4	-87	.2	-4.2
11.1103	-2.5	3.6	-87	1.8	-3.7
11.1153	-4.1	1.8	-87	3.0	-2.4
11.1200	-4.6	-.4	-87	3.4	-.1
11.1250	-3.9	-2.7	-87	2.8	.1
11.1300	-2.2	-4.3	-87	1.5	2.2
11.1350	.2	-4.9	-87	-.2	2.5
11.1397	2.4	-4.2	-87	-1.9	2.1
11.1447	4.1	-2.5	-87	-3.1	.8
11.1497	4.7	-.1	-87	-3.5	-1.0

TABLE II.- SAMPLE OF "FLIGHT" DATA FOR CASE 2

Time, sec	a_Y, g units	a_Z, g units	p, rad/sec	q, rad/sec	r, rad/sec
1678.0209	-1.9	2.0	19	3.9	1.6
1678.0259	-1.7	1.9	19	4.7	2.4
1678.0309	-1.3	1.7	19	5.4	3.2
1678.0359	-1.0	1.4	19	6.0	3.7
1678.0409	-.6	1.0	19	6.4	4.1
1678.0456	-.2	.5	19	6.6	4.3
1678.0512	.3	-.1	19	6.6	4.4
1678.0562	.6	-.7	19	6.4	4.4
1678.0612	.9	-1.3	19	5.9	4.2
1678.0662	1.0	-1.7	19	5.3	3.9
1678.0712	1.1	-2.1	19	4.4	3.6
1678.0763	1.1	-2.5	19	3.4	3.2
1678.0812	1.0	-2.7	19	2.2	2.8
1678.0862	.9	-2.8	19	.9	2.3
1678.0912	.8	-2.9	19	-.5	1.9
1678.0956	.7	-2.9	19	-1.7	1.6
1678.1006	.5	-2.9	19	-3.1	1.3
1678.1056	.3	-2.7	19	-4.3	1.1
1678.1112	.2	-2.4	19	-5.6	.8
1678.1162	0	-2.0	19	-6.5	.7
1678.1212	-.1	-1.6	19	-7.2	.6
1678.1262	-.2	-.9	19	-7.7	.6
1678.1312	-.2	-.3	19	-7.9	.5
1678.1362	-.2	.4	19	-7.9	.4
1678.1412	-.1	1.1	19	-7.6	.3
1678.1462	.1	1.7	19	-7.1	.2
1678.1506	.3	2.1	19	-6.5	0

TABLE III.- SAMPLE OF "FLIGHT" DATA FOR CASE 3

Time, sec	a_Y, g units	a_Z, g units	p, rad/sec	q, rad/sec	r, rad/sec
1678.0192	1.7	-0.8	19	2.9	3.3
1678.0236	1.8	-1.0	19	1.3	2.8
1678.0275	1.8	-1.2	19	0	2.2
1678.0323	1.8	-1.3	19	-1.9	1.5
1678.0373	1.8	-1.2	19	-3.8	.7
1678.0423	1.8	-1.0	19	-5.6	-.1
1678.0473	1.7	-.7	19	-7.3	-.9
1678.0523	1.6	-.2	19	-8.8	-1.7
1678.0580	1.4	.6	19	-10.2	-2.5
1678.0630	1.2	1.4	19	-11.1	-3.2
1678.0680	1.0	2.1	19	-11.7	-3.8
1678.0730	.9	2.8	19	-12.0	-4.4
1678.0780	.8	3.3	19	-11.8	-5.0
1678.0830	.7	3.8	19	-11.2	-5.6
1678.0880	.7	4.2	19	-10.2	-6.1
1678.0930	.8	5.0	19	-8.9	-6.7
1678.0980	.9	5.7	19	-7.3	-7.3
1678.1030	1.0	6.2	19	-5.5	-7.8
1678.1080	1.1	6.5	19	-3.5	-8.4
1678.1130	1.1	6.6	19	-1.5	-8.9
1678.1167	1.1	6.6	19	.1	-9.3
1678.1217	1.1	6.3	19	2.1	-9.8
1678.1267	1.0	5.8	19	4.0	-10.3
1678.1317	.8	5.2	19	5.7	-10.6
1678.1367	.5	4.5	19	7.2	-10.8
1678.1417	.3	4.0	19	8.3	-10.9
1678.1455	0	3.7	19	9.0	-10.9

TABLE IV.- SAMPLE OF REFERENCE 2 FLIGHT DATA

Time, sec	a_Y, g units	a_Z, g units	p, rad/sec	q, rad/sec	r, rad/sec
443.89	3.11	0.60	12	0.5	0.5
443.91	2.83	-.26	12	.8	-.2
443.93	2.06	-1.03	12	.7	-.9
443.95	1.16	-1.63	12	.4	-1.3
443.97	.26	-1.69	12	0	-1.4
443.99	-.55	-1.31	12	-.5	-1.5
444.01	-1.29	-.64	12	-.9	-1.4
444.03	-1.61	.23	12	-1.3	-1.0
444.05	-1.67	1.26	12	-1.5	-.6
444.07	-1.45	2.25	12	-1.5	0
444.09	-.55	2.99	12	-1.2	.3
444.11	.45	3.20	12	-.6	.5
444.13	1.31	2.70	12	0	.6
444.15	2.02	1.81	12	.7	.5
444.17	2.08	.78	12	1.2	.1
444.19	1.79	-.05	12	1.5	-.4
444.21	1.25	-1.10	12	1.4	-1.0
444.23	.40	-1.66	12	1.2	-1.3
444.25	-.56	-1.88	12	.7	-1.4
444.27	-1.51	-1.81	12	.3	-1.4
444.29	-2.48	-1.22	12	-.2	-1.3
444.31	-3.04	-.31	12	-.6	-.8
444.33	-2.94	.99	12	-.8	-.2
444.35	-2.21	1.99	12	-.8	.4
444.37	-1.19	2.24	12	-.4	1.0
444.39	-.04	2.14	12	0	1.3
444.41	.76	1.59	12	.6	1.3

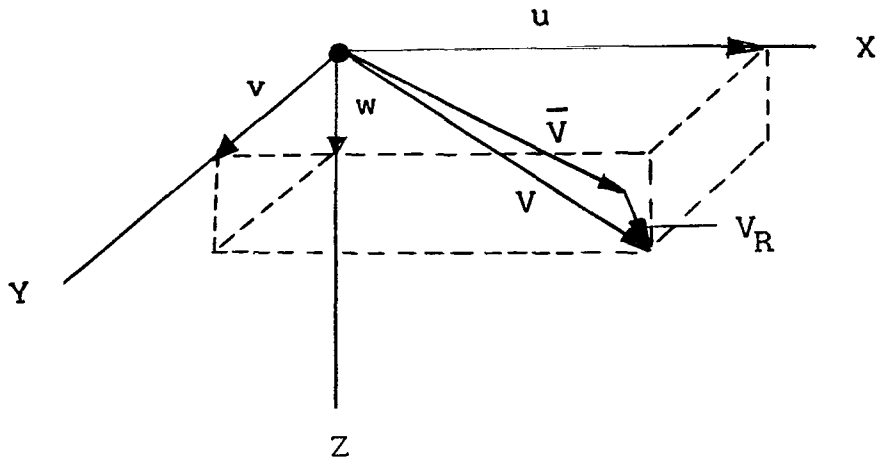

(a) Velocity components system.

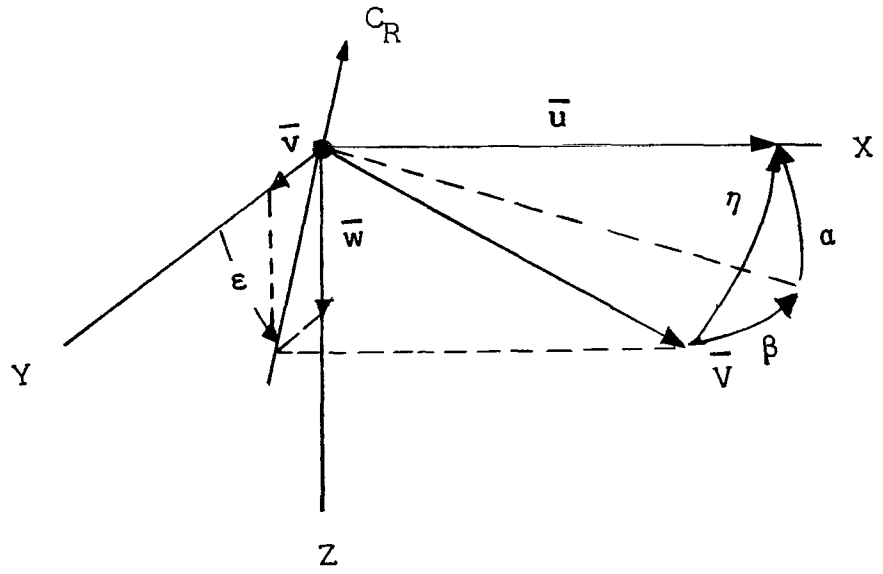

(b) Aerodynamic angle system.

Figure 1.- Body-axis system orientation.

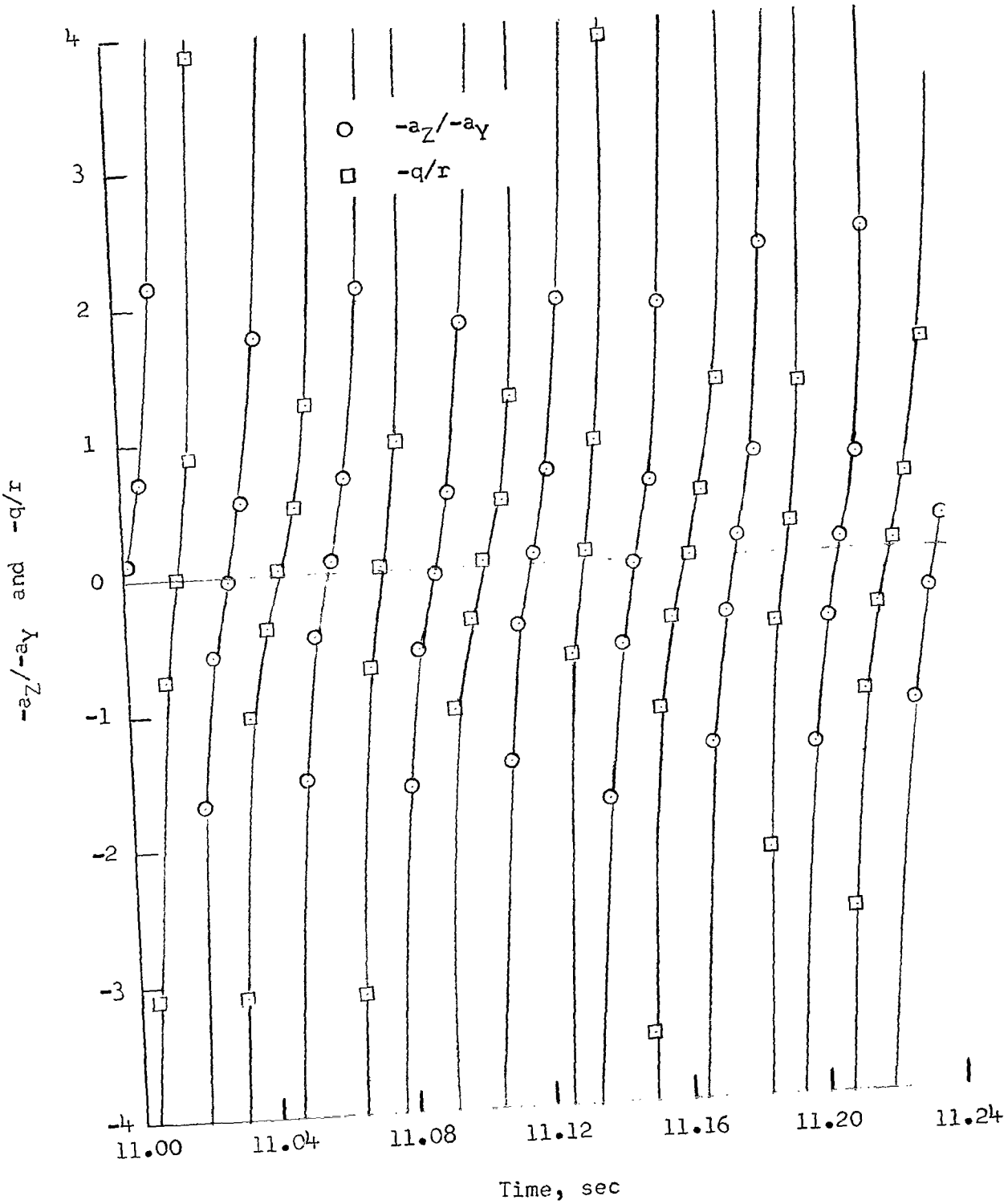

Figure 2.- Time histories of $-a_Z/-a_Y$ and $-q/r$ for case 1.

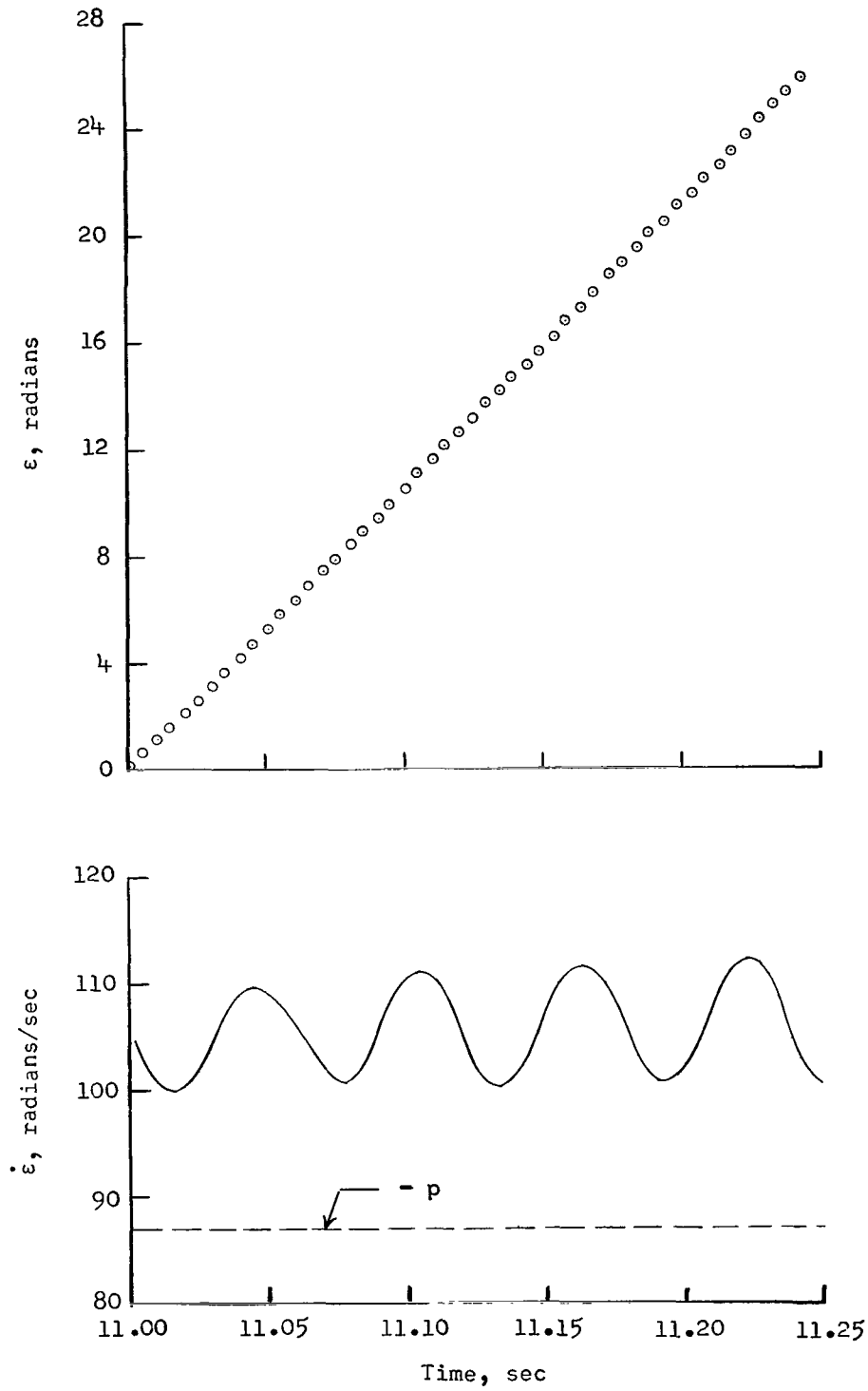

Figure 3.- Time histories of ε and $\dot{\varepsilon}$ for case 1.

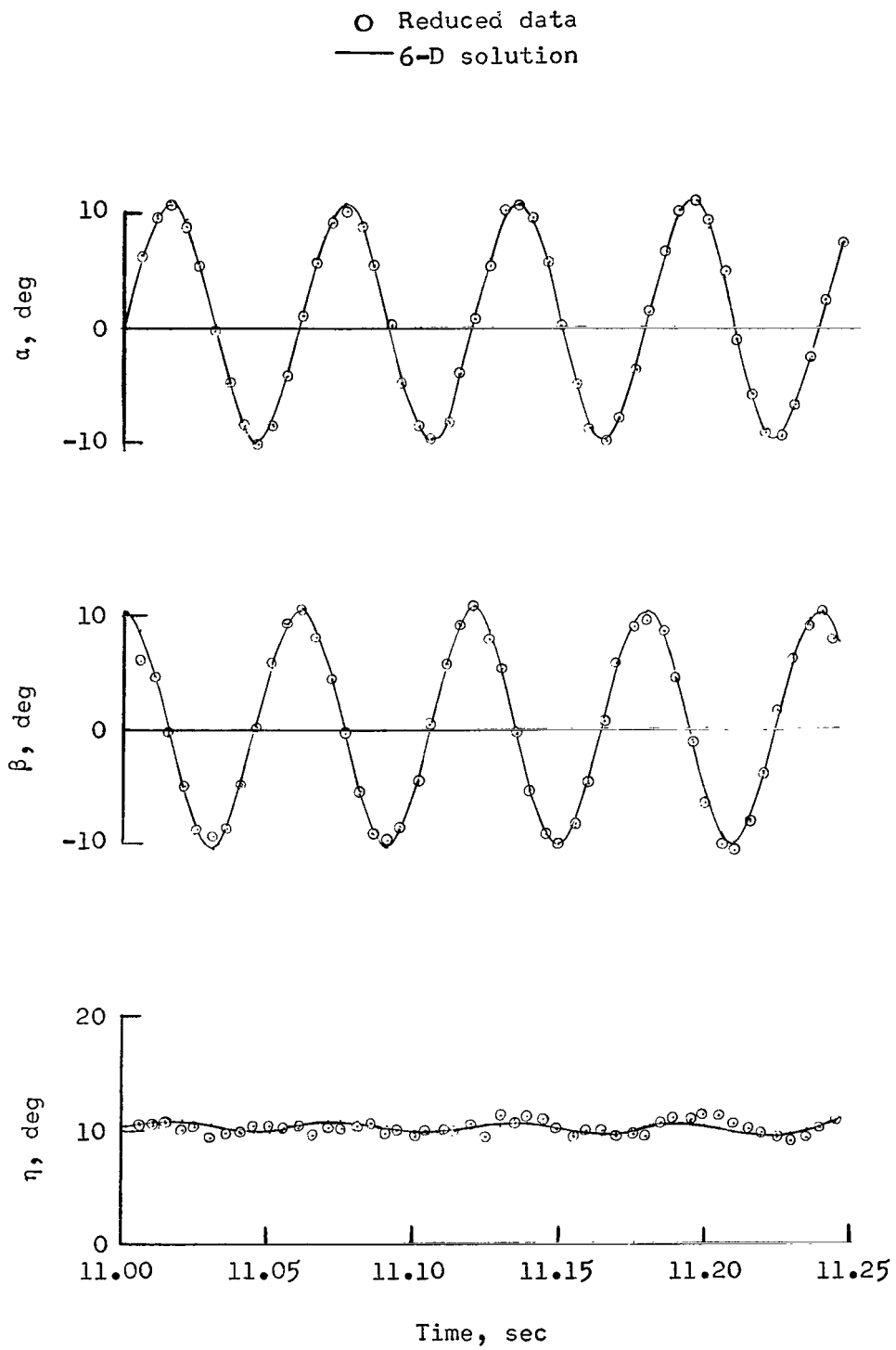

Figure 4.- Time histories of α, β, and η for case 1.

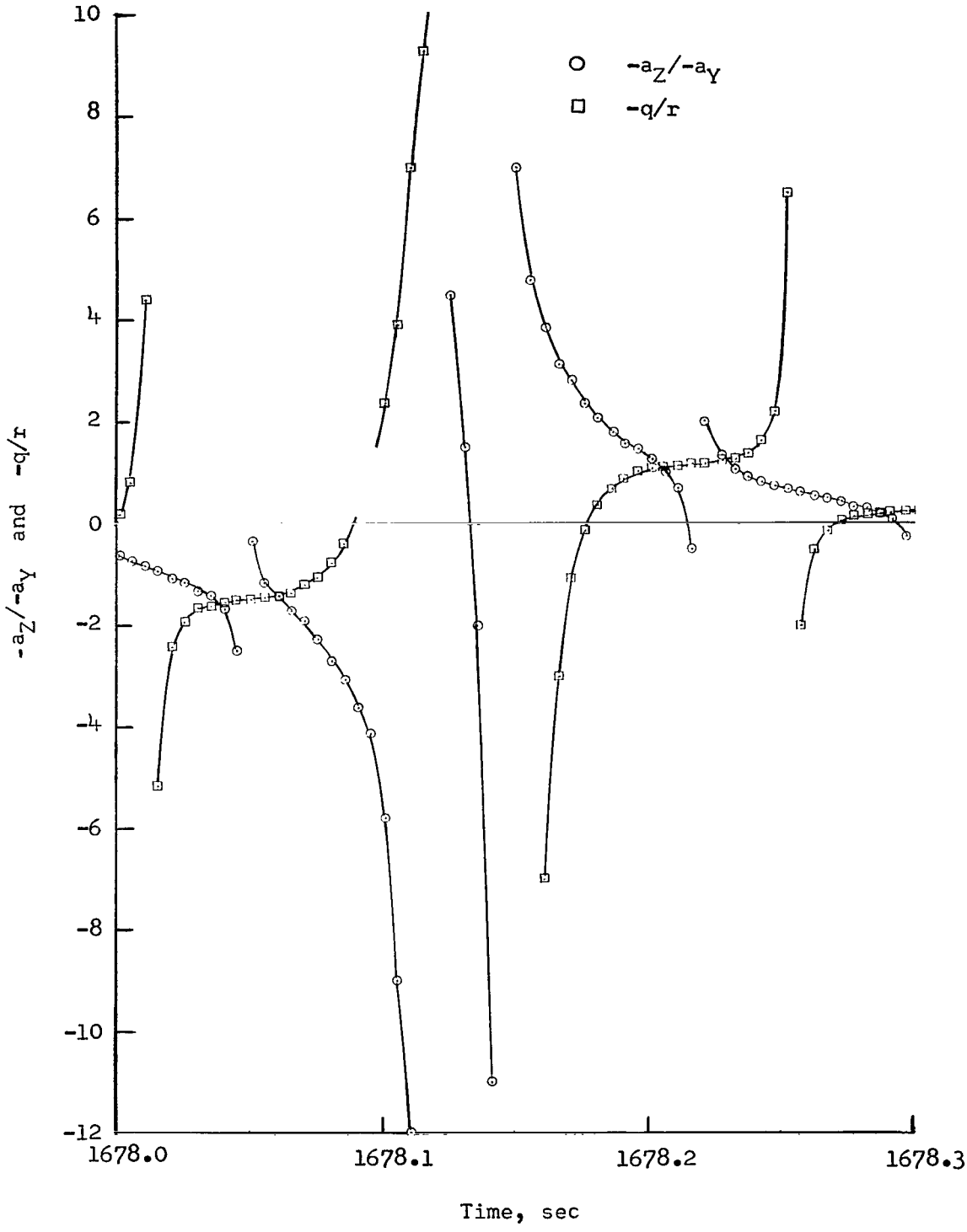

Figure 5.- Time histories of $-a_Z/-a_Y$ and $-q/r$ for case 2.

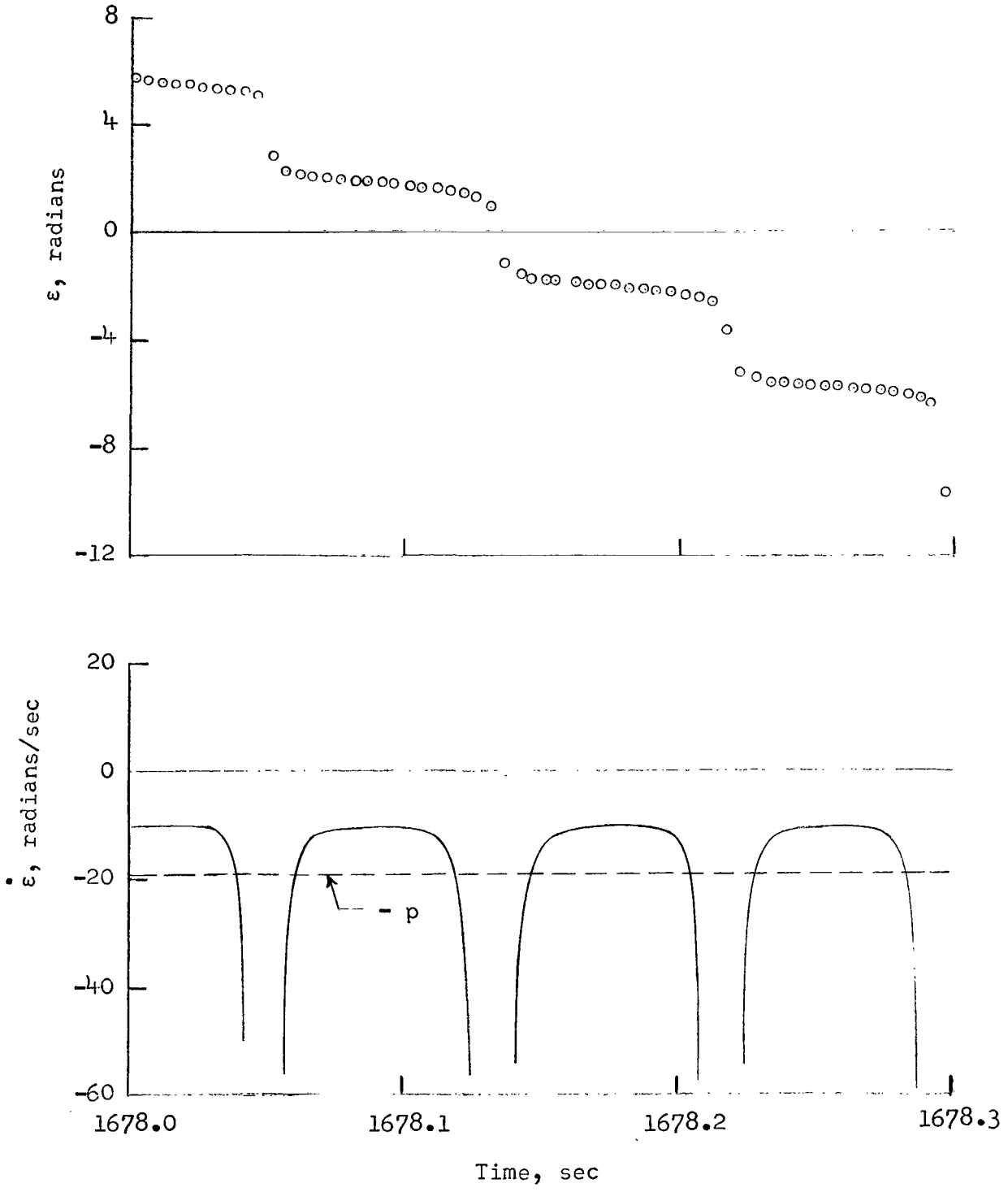

Figure 6.- Time histories of ε and $\dot{\varepsilon}$ for case 2.

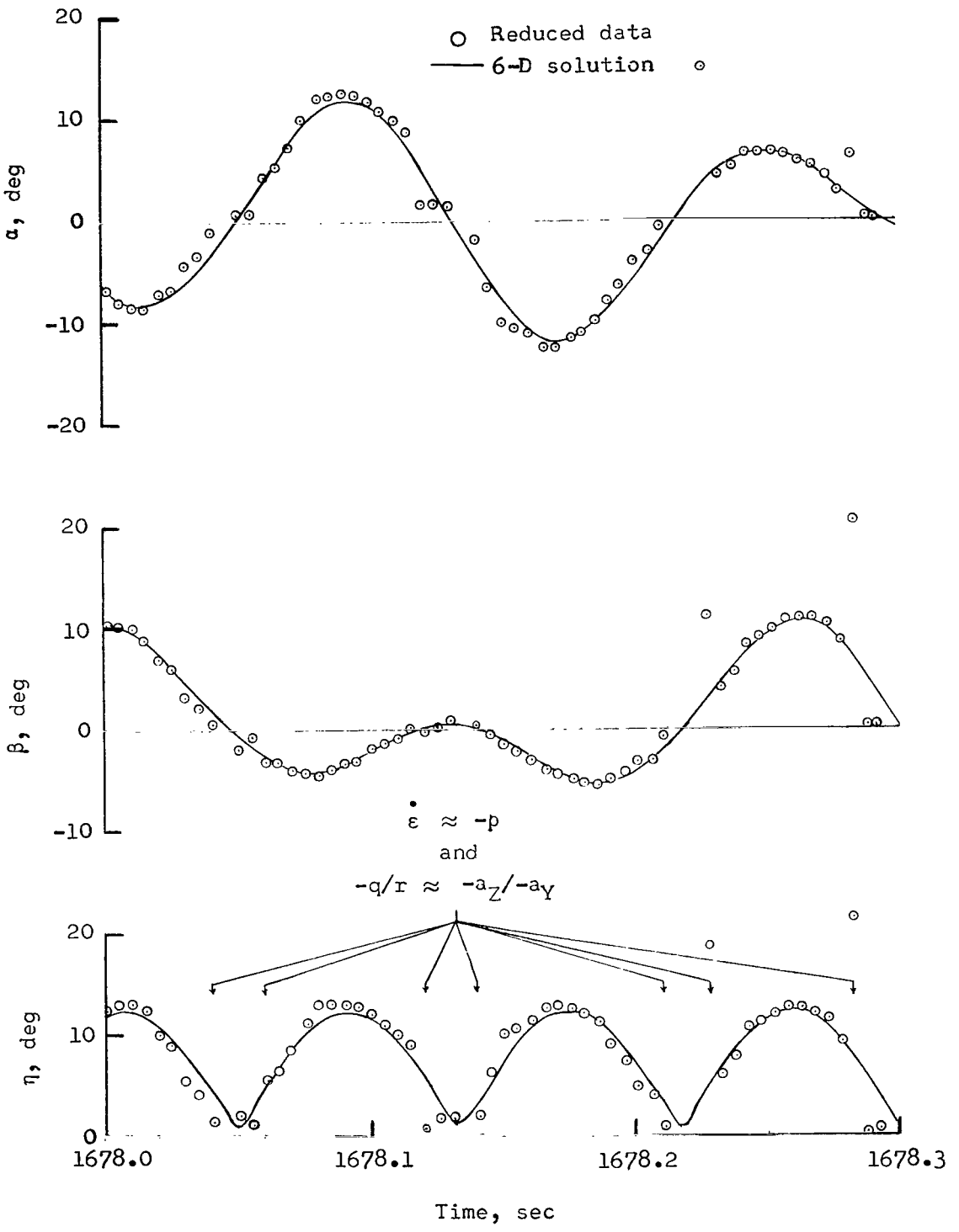

Figure 7.- Time histories of α, β, and η for case 2.

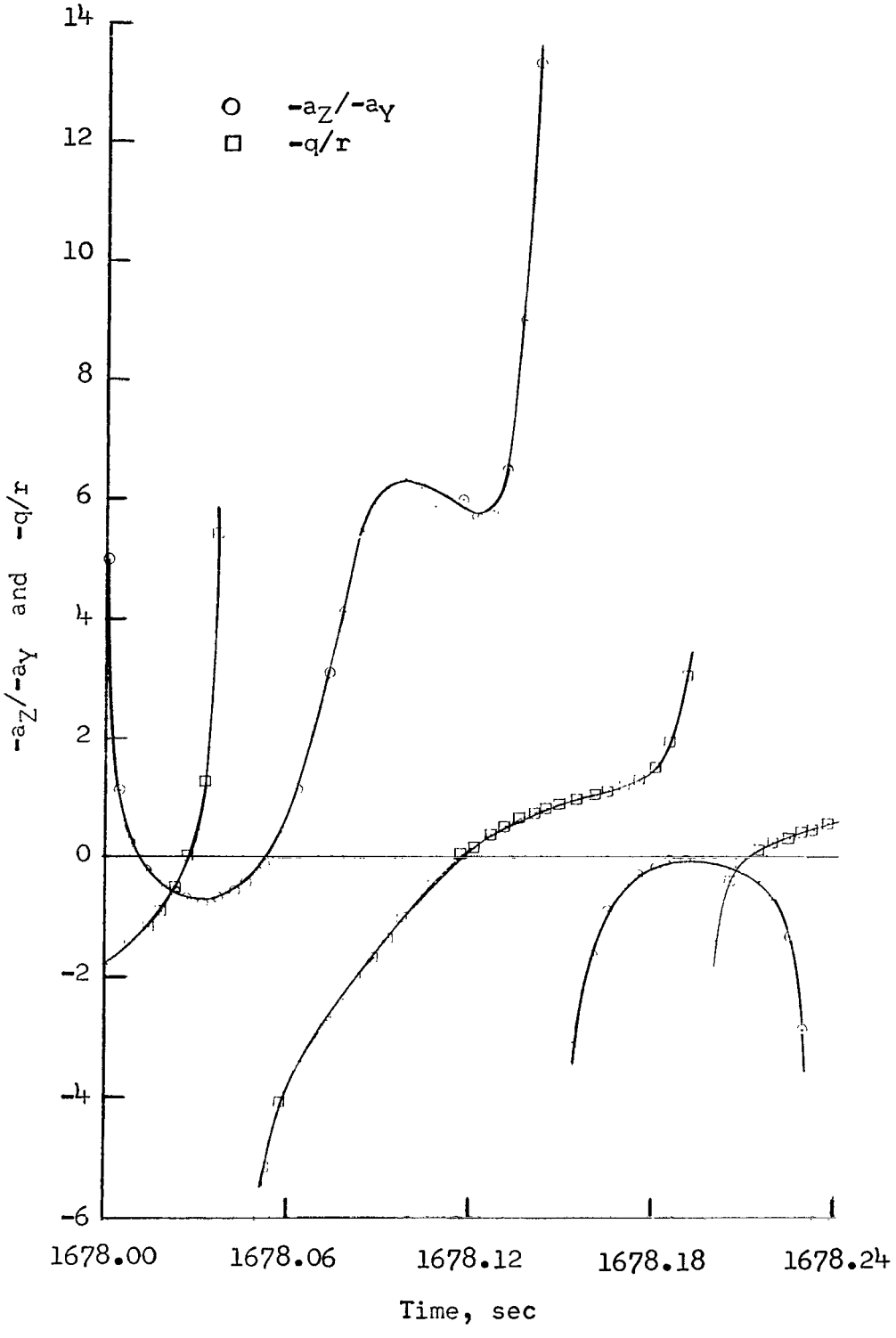

Figure 8.- Time histories of $-a_Z/-a_Y$ and $-q/r$ for case 3.

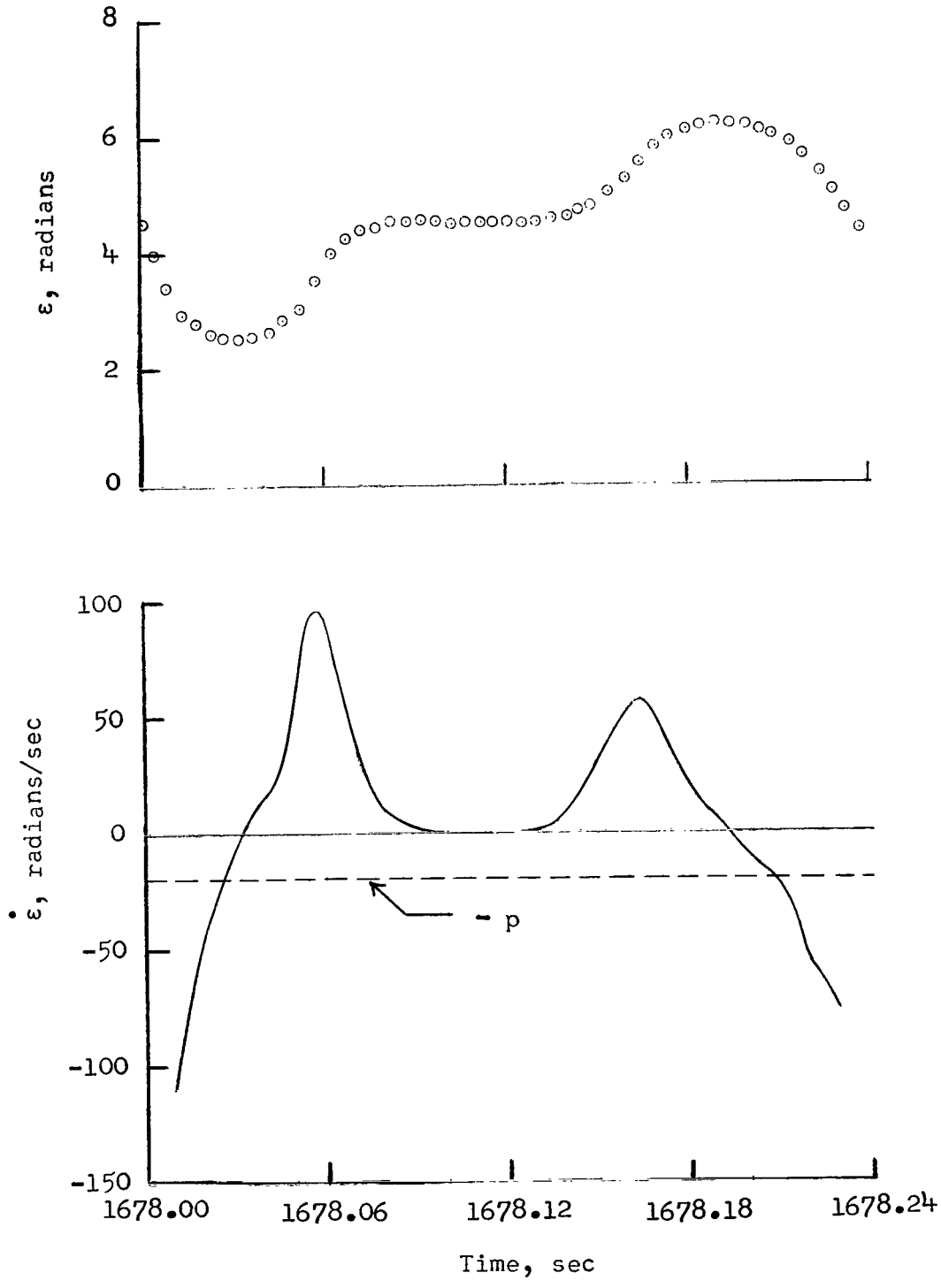

Figure 9.- Time histories of ε and $\dot{\varepsilon}$ for case 3.

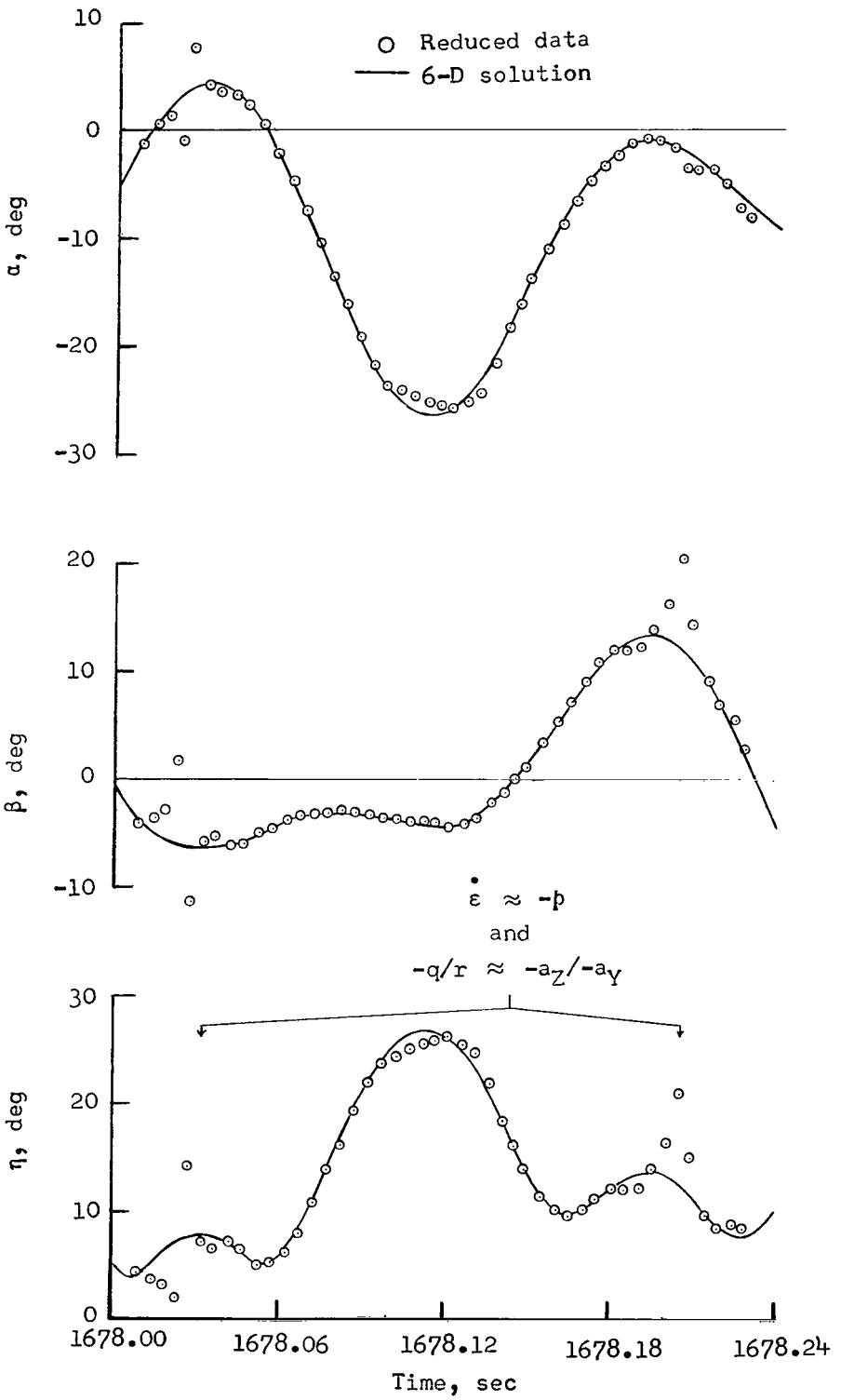

Figure 10.- Time histories of α, β, and η for case 3.

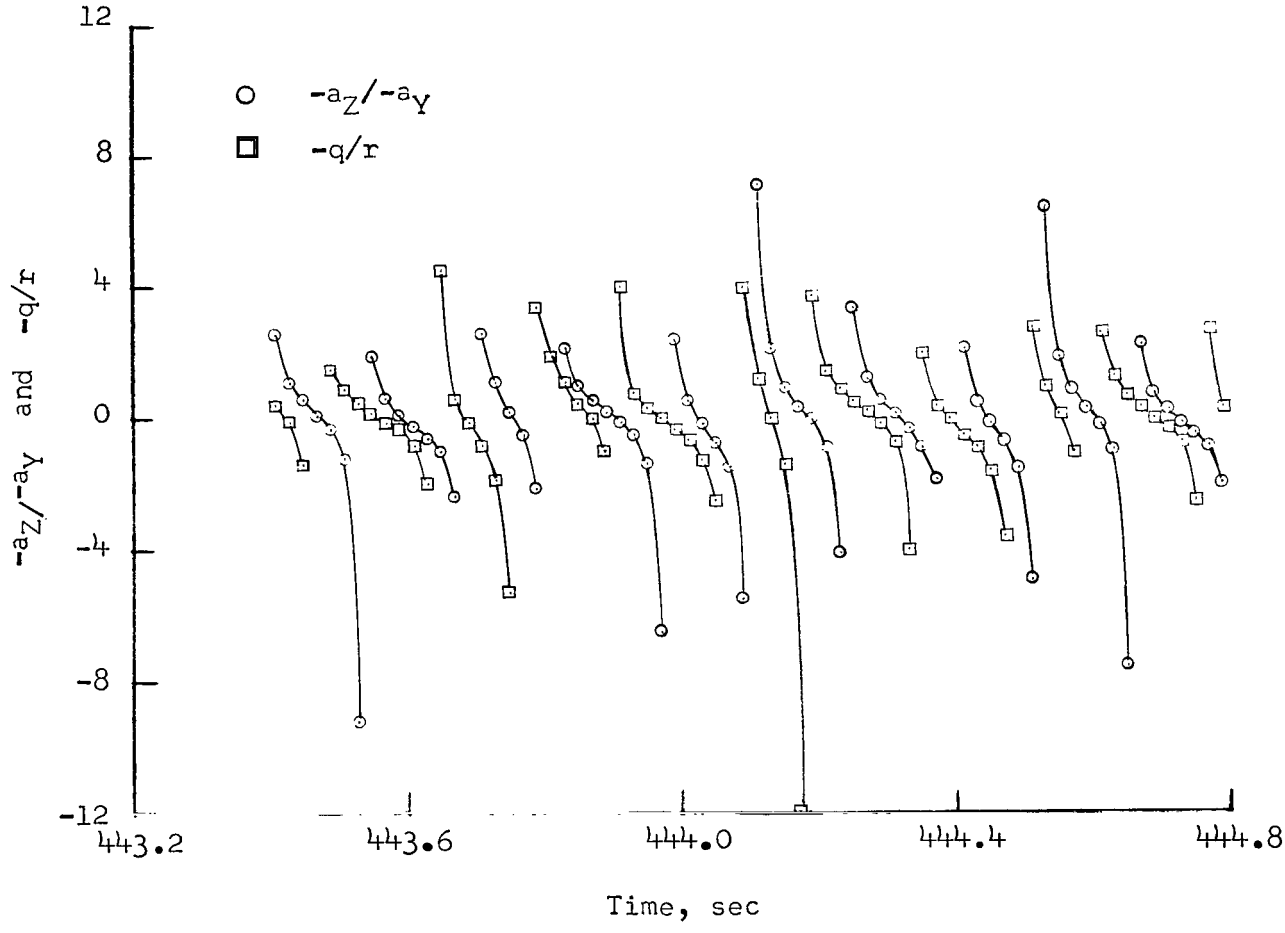

Figure 11.- Time histories of $-a_Z/-a_Y$ and $-q/r$ for reference 2 data.

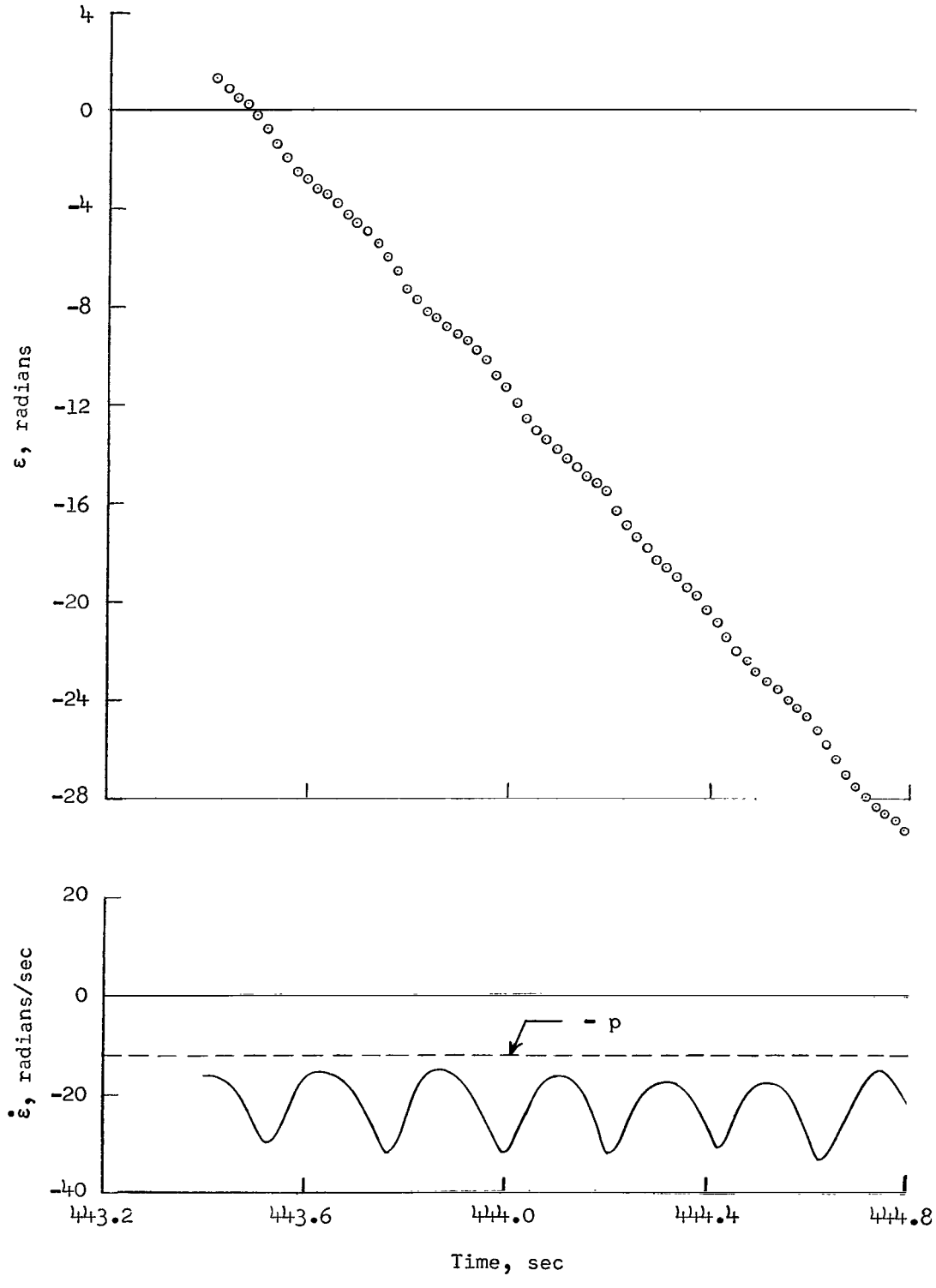

Figure 12.- Time histories of ε and $\dot{\varepsilon}$ for reference 2 data.

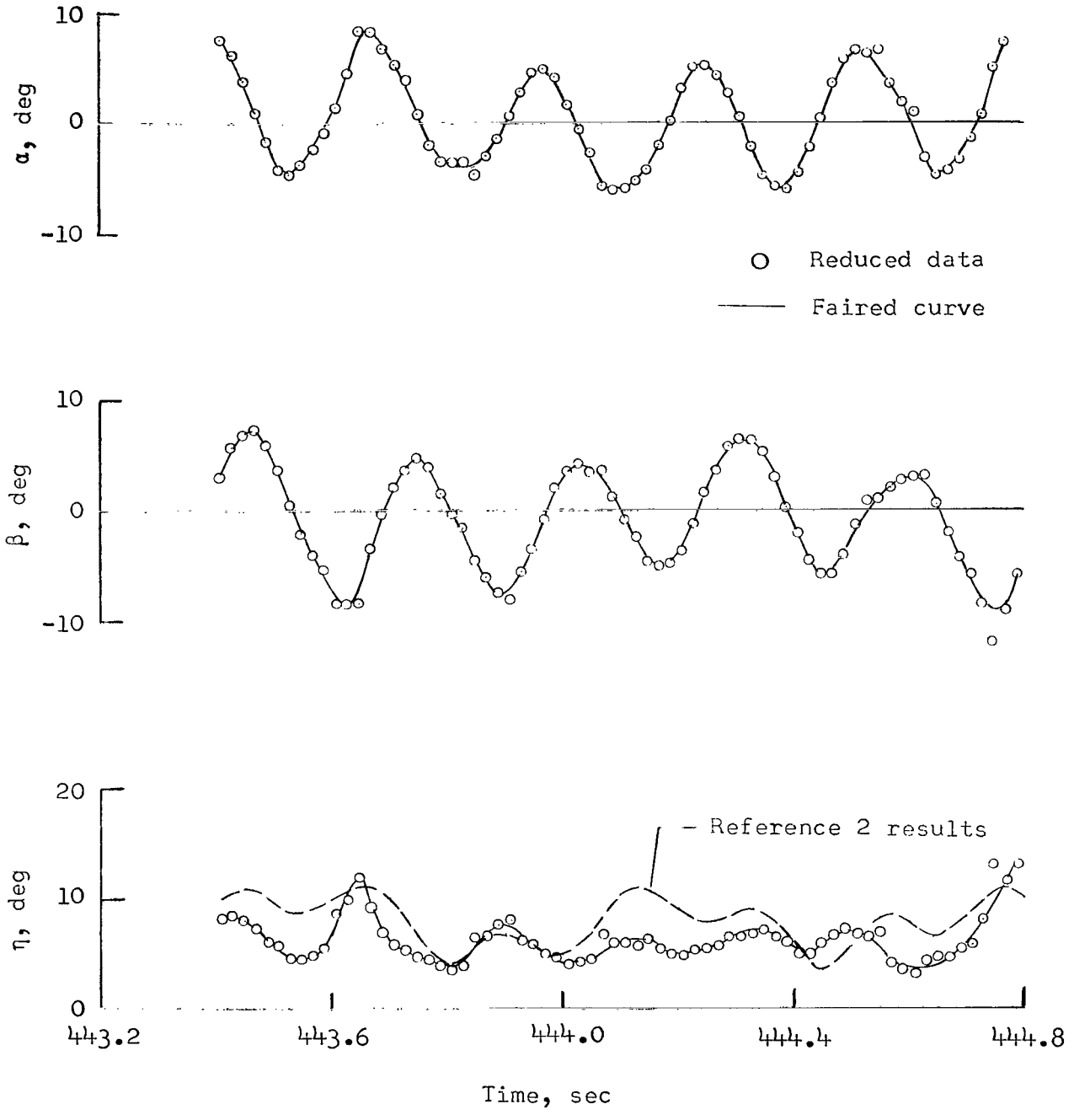

Figure 13.- Time histories of α, β, and η for reference 2 data.

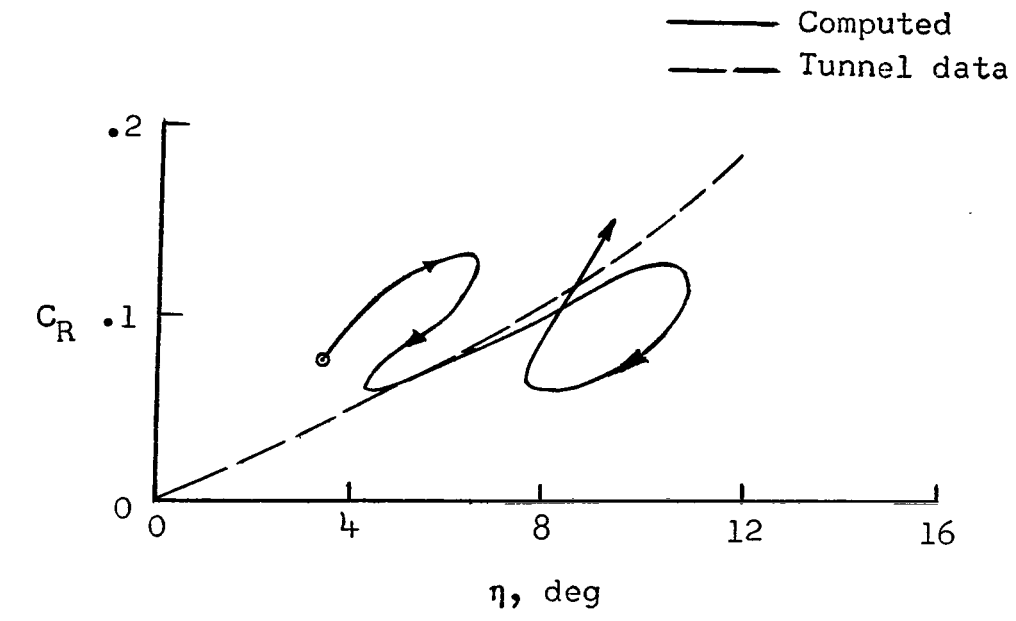

(a) Results from reference 2 (t = 443.81 to 444.35 sec).

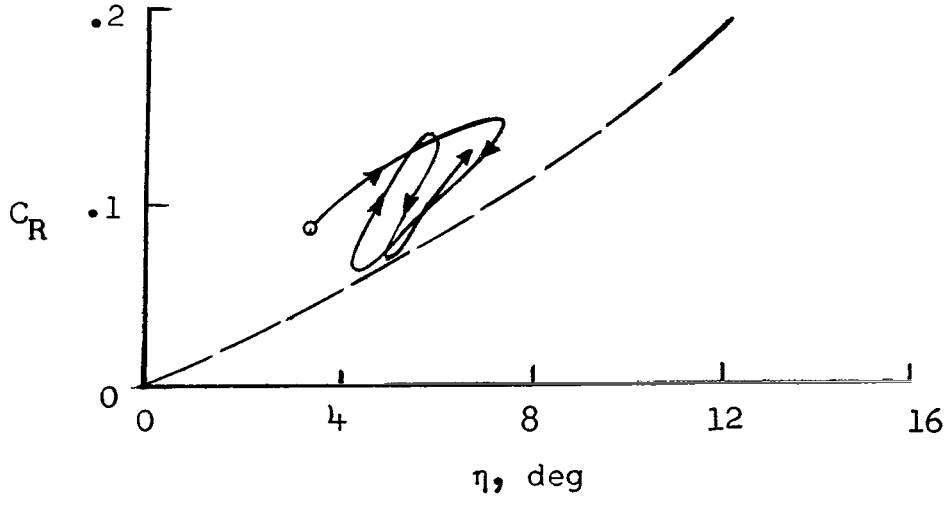

(b) Results using figure 13 data (t = 443.81 to 444.35 sec).

Figure 14.- Comparison between wind-tunnel and computed flight resultant force coefficients.

"The aeronautical and space activities of the United States shall be conducted so as to contribute . . . to the expansion of human knowledge of phenomena in the atmosphere and space. The Administration shall provide for the widest practicable and appropriate dissemination of information concerning its activities and the results thereof."

—NATIONAL AERONAUTICS AND SPACE ACT OF 1958

NASA SCIENTIFIC AND TECHNICAL PUBLICATIONS

TECHNICAL REPORTS: Scientific and technical information considered important, complete, and a lasting contribution to existing knowledge.

TECHNICAL NOTES: Information less broad in scope but nevertheless of importance as a contribution to existing knowledge.

TECHNICAL MEMORANDUMS: Information receiving limited distribution because of preliminary data, security classification, or other reasons.

CONTRACTOR REPORTS: Technical information generated in connection with a NASA contract or grant and released under NASA auspices.

TECHNICAL TRANSLATIONS: Information published in a foreign language considered to merit NASA distribution in English.

TECHNICAL REPRINTS: Information derived from NASA activities and initially published in the form of journal articles.

SPECIAL PUBLICATIONS: Information derived from or of value to NASA activities but not necessarily reporting the results of individual NASA-programmed scientific efforts. Publications include conference proceedings, monographs, data compilations, handbooks, sourcebooks, and special bibliographies.

Details on the availability of these publications may be obtained from:

SCIENTIFIC AND TECHNICAL INFORMATION DIVISION

NATIONAL AERONAUTICS AND SPACE ADMINISTRATION

Washington, D.C. 20546